

# Scaling in large area field emitters and the emission dimension

Rashbihari Rudra<sup>1,2</sup> and Debabrata Biswas<sup>1,2, a)</sup>

<sup>1)</sup>*Bhabha Atomic Research Centre, Mumbai 400 085, INDIA*

<sup>2)</sup>*Homi Bhabha National Institute, Mumbai 400 094, INDIA*

Electrostatic shielding is an important consideration for large area field emitters (LAFE) and results in a distribution of field enhancement factors even when the constituent emitters are identical. Ideally, the mean and variance together with the nature of the distribution should characterize a LAFE. In practice however, it is generally characterized by an effective field enhancement factor obtained from a linear fit to a Fowler-Nordheim plot of the I-V data. An alternate characterization is proposed here based on the observation that for a dense packing of emitters, shielding is large and LAFE emission occurs largely from the periphery, while well separated emitter tips show a more uniform or 2-dimensional emission. This observation naturally leads to the question of the existence of an emission-dimension,  $D_e$  for characterizing LAFEs. We show here that the number of patches of size  $L_P$  in the ON-state (above average emission) scales as  $N(L_P) \sim L_P^{-D_e}$  in a given LAFE. The exponent  $D_e$  is found to depend on the applied field (or voltage) and approaches  $D_e = 2$  asymptotically.

## I. INTRODUCTION

A large area field emitter (LAFE) holds much promise as a cold source of electrons<sup>1-7</sup>. A typical LAFE consists of several thousands of individual field emitters packed together in a finite area  $\mathcal{A}$ . The current density from a LAFE is limited by two counter-acting effects. An increase in the number of emitters in  $\mathcal{A}$  results in more emitting tips. This however results in enhanced shielding between individual emitters which reduces the local field on individual tips. Thus, the number of emitters can be increased by packing more of them but beyond a point, this is counter-productive as individual contributions reduce sharply on account of shielding<sup>11</sup>. To further complicate matters, the ideal packing density itself depends on the applied field and even the distance between the tip and the anode<sup>8-16</sup>.

As shielding is non-uniform in any finite-sized LAFE, whether ordered or random, the field enhancement factor,  $\gamma$ , differs from tip to tip even if all emitters are identical in all respects. Thus, there exists a distribution  $f(\gamma)$  of enhancement factors  $\gamma$  at a given packing density (emitters per unit area) resulting in some interesting behavior. As a thumb rule, the periphery of a LAFE generally suffers minimal shielding and contributes more to the net current especially at higher packing densities while at higher applied fields or lower packing densities, even the emitters that are more centrally-located contribute to the current and start becoming visible in a current heat map.

The complexity of a LAFE leads to difficulties in its characterization. Unlike a single emitter where the apex field enhancement factor,  $\gamma$  and the apex radius  $R_a$  are in-principle sufficient to determine the I-V characteristics, a LAFE is conventionally characterized by an effective field enhancement factor and the notional emission area. In most instances however, the FN-plot is non-linear and the effective enhancement factor,  $\gamma_c$ , obtained

from the slope of the regression line fitted to the experimental FN plot, is a poor representation of the LAFE. Instead, the low and high field fits can be used to construct a 2-emitter class model with distinct enhancement-factors<sup>17,18</sup>. There is much however that needs to be understood since we are really dealing with a distribution of enhancement factors in a typical LAFE<sup>11,19,20</sup>

Even in case of a single emitter, the pre-exponential factor in the empirical expression for net current<sup>21</sup>

$$I_S = A_s E_0^{k_s} e^{-B_s/E_0} \quad (1)$$

is not entirely a settled issue. For a flat emitter of area  $A$ ,  $I_S = A J_{MG}$ , where  $J_{MG}$  is the Murphy-Good current density<sup>22-30</sup>. Thus,  $k_s = 2 - \nu$  where  $\nu = \eta/6$  with  $\eta \approx 9.836$  (eV)<sup>1/2</sup> $\phi^{-1/2}$ . When, the emitter is curved and the local field varies on its surface,  $I_S = \int_A J_{MG} dA$ . For generic smooth endcap shapes<sup>31,32</sup>, the integration can be performed and it is known<sup>33</sup> that  $k_s \approx 3 - \nu$ . There are exceptions however, most notably for the hemisphere on a cylindrical post model. The value of  $k_s$  has an important bearing on the experimental characterization of single emitter tips, especially the notional emission area defined as  $I_S/J_{MG}^{apex}$ . Thus, while the apex enhancement factor of a single tip is largely unaffected by the choice of  $k_s$  and can be determined from the slope of an FN-plot, the emission area depends on the choice of  $k_s$ .

A LAFE consists of a collection of single emitters, each with a distinct apex field enhancement factor. The net LAFE current  $I_L$ , can thus be expressed as

$$I_L = \sum_{i=1}^N A_s^i E_0^{k_s} e^{-B_s^i/E_0} = E_0^{k_s} \left( \sum_{i=1}^N A_s^i e^{-B_s^i/E_0} \right) \quad (2)$$

assuming that they have identical shapes. The terms in the bracket distinguishes a LAFE from a single emitter. If all the  $N$  emitters are identical and well separated,  $A_s^i$  and  $B_s^i$  would be the same for all emitters so that the net current  $I_L \approx I_S N = I_S \rho \mathcal{A}$  where  $\rho$  is the number of

<sup>a)</sup>Electronic mail: dbiswas@barc.gov.in

emitters per unit area and  $\mathcal{A}$  is the geometric area of the LAFE.

If the LAFE is not as sparse,  $A_S^i$  and  $B_S^i$  may be distinct for each emitter and it is likely that in writing<sup>34</sup>

$$I_L = A_L E_0^{k_L} e^{-B_L/E_0} \quad (3)$$

as in the single emitter case,  $k_L \neq k_S$ . As a matter of fact, it is not apparent that the slope  $B_L$  in an FN plot is directly related to the enhancement factor of a LAFE even though it is commonly used to extract the characteristic enhancement factor(s). There are thus additional unresolved issues in dealing with a LAFE.

We propose here a markedly different approach to LAFE characterization based on the observation that the glow pattern of a LAFE (the heat map) can vary from seemingly 1-dimensional peripheral emission at low applied fields or high packing densities, to the more uniform seemingly 2-dimensional emission at higher fields or lower packing densities. The question that we therefore address is whether there exists any scaling behavior in a given LAFE that can capture the essence of the glow pattern typical of a LAFE. More specifically, we wish to investigate whether the number of patches (or covers) of size  $L_P$  that outshines (ON state) the average behavior in a given LAFE, scales as  $L_P^{-D_e}$ . If such a relationship does indeed hold, it is also of interest to determine how the exponent  $D_e$  varies with  $E_0$ .

The information contained in the emission dimension can be useful in various ways and can complement the I-V data. It can for instance indicate the optimal emitter density and operating voltages that can lead to uniform emission or even serve as a guide in designing a device.

The paper is organized as follows. In Section II, we shall outline the methodology used for the scaling study including a brief sketch of LAFE simulation. This is followed by the results on scaling and finally a summary with a brief discussion on the experimental realization of the scaling exponent.

## II. SIMULATION METHODOLOGY

Simulation of a LAFE having thousands of randomly placed individual emitters is central to the scaling studies that we wish to perform. Clearly, such a massive task cannot be performed using ‘exact’ numerical methods such as finite element or boundary element techniques as it would require enormous resources. An alternate approximate technique that is now well-tested, is based on the line charge model. It involves the linear line charge density and is applicable to hemi-ellipsoidal emitters. It is reasonably accurate when the spacing between emitters is not too small compared to its height. A generalization for other emitter shapes involving nonlinear line charge density leads to the hybrid model for simulation of a general LAFE. We shall hereafter limit our discussion

to hemi-ellipsoidal emitters without any loss of generality.

### A. Current from a collection of emitters

Consider a large area field emitter comprising of  $N$  identical hemi-ellipsoidal shaped emitters, each placed at  $(x_i, y_i)$ ,  $i = 1, N$ . The apex field enhancement factor  $\gamma$  is defined as the ratio of the local field at the apex,  $E_a$  and the applied or macroscopic field  $E_0$ , i.e.  $\gamma = E_a/E_0$ . It is a geometric quantity and depends principally on the ratio of its height  $h$  and the apex radius of curvature,  $R_a$ <sup>10,35,36</sup>. For a collection of  $N$  emitters, the field enhancement depends on the degree of shielding and the proximity of the anode and a comprehensive modular theory has been developed which provides an approximate value of the enhancement of an  $i^{\text{th}}$  emitter in the LAFE<sup>10-15</sup>. If the anode is considered to be far away, shielding effects dominate and the apex field enhancement at the  $i^{\text{th}}$  emitter is given by<sup>11</sup>,

$$\gamma_i \simeq \frac{2h/R_a}{\ln(4h/R_a) - 2 + \alpha_{S_i}} \quad (4)$$

where  $\alpha_{S_i} = \sum_{j \neq i} (\lambda_j/\lambda_i) \alpha_{S_{ij}} \simeq \sum_{j \neq i} \alpha_{S_{ij}}$  and

$$\alpha_{S_{ij}} = \frac{1}{\delta_{ij}} \left[ 1 - \sqrt{1 + 4\delta_{ij}^2} \right] + \ln \left| \sqrt{1 + 4\delta_{ij}^2} + 2\delta_{ij} \right|$$

with  $\delta_{ij} = h/\rho_{ij}$ ,  $\rho_{ij} = [(x_i - x_j)^2 + (y_i - y_j)^2]^{1/2}$  being the distance between the  $i^{\text{th}}$  and  $j^{\text{th}}$  emitter on the cathode plane. In the above,  $\lambda$  is the slope of the line charge density  $\Lambda(z)$  (i.e.  $\Lambda(z) = \lambda z$ ), obtained by projecting the surface charge density along the emitter axis<sup>37</sup>. The approximation  $\lambda_i/\lambda_j \approx 1$  is found to be reasonable so long as the pair of emitters are not too close compared to their height. Note that under this approximation, the shielding factor,  $\alpha_{S_i}$  is a purely geometric quantity. The predictions of Eq. (4) have been well tested<sup>13</sup> and found to be accurate if the emitters are not too close to each other.

It is clear that if the emitter locations are randomly distributed,  $\{\alpha_{S_i}\}$  and hence  $\{\gamma_i\}$  are distinct. There is thus a distribution of enhancement factors which can be determined on evaluating  $\{\gamma_i\}$  using Eq. (4). If the mean inter-pin separation  $c$  is smaller than the height  $h$  of the emitters, the distribution is skewed to the right and emission is generally observed from the periphery. On the other hand, when  $c > 2.5h$ , shielding has negligible effect on the local field enhancement.

The field enhancement factors  $\{\gamma_i\}$  together with the apex radius of curvature  $R_a$  can be used to determine the total LAFE current,  $I_L$  as<sup>33</sup>

$$I_L \approx \sum_{i=1}^N 2\pi R_a^2 g_i J_{MG}^i \quad (5)$$

where the area factor  $g_i$  is

$$g_i = \frac{\gamma_i E_0}{B_{\text{FN}} \phi^{3/2}} \frac{1}{(1 - f_i/6)} \quad (6)$$

and the current density  $J_{MG}$  is<sup>25,27</sup>

$$J_{MG}^i = \frac{A_{\text{FN}} (\gamma_i E_0)^2}{\phi t_F^2} \exp\left(-\nu_F^i B_{\text{FN}} \phi^{3/2} / (E_0 \gamma_i)\right) \quad (7)$$

where,  $A_{\text{FN}} = 1.541434 \times 10^{-6} \text{ A eV V}^{-2}$  and  $B_{\text{FN}} = 6.830890 \text{ eV}^{-3/2} \text{ V nm}^{-1}$  are the first and second Fowler-Nordheim constants,  $\phi$  is the local work function of the emitting surface,  $\nu_F^i = 1 - f_i + (f_i/6) \ln(f_i)$ ,  $t_F = 1 + f_i/9 - (f_i/18) \ln(f_i)$  and  $f_i \approx 1.44 \gamma_i E_0 / \phi^2$ .

Eq. (5) can be used to determine the current from a collection of N-emitters. It is particularly suited for the scaling study which requires determination of the current from a patch of size  $L_P$  from any part of the LAFE. Throughout this study, we shall consider the work-function  $\phi$  to be uniform over the tip having a value 4.5eV. It is assumed that the work function remains constant throughout the simulation or experiment as the case may be.

## B. The scaling methodology

Consider a LAFE of an arbitrary shape having an area  $\mathcal{A}$ . Geometrically, it can be covered by  $N_P$  non-overlapping square patches of size  $L_P$ . Since the LAFE itself is a 2-dimensional structure,  $N_P \sim L_P^{-2}$ . This can be seen explicitly by writing  $N_P = \mathcal{A}/L_P^2$ . Thus, we are clearly not dealing with a geometric fractal.

Each patch covering the LAFE carries a net current  $I_P$ . Since the patches are non-overlapping,  $I_L = \sum I_P$ . The average current density of the LAFE is  $J_L = I_L/\mathcal{A}$  and this serves as a useful parameter in deciding whether a patch is emitting more than the background (ON state) or less (OFF state). Thus, if  $I_{P_k} \geq \alpha J_L L_P^2$ , the  $k^{\text{th}}$  patch is considered to be in the ON-state and assigned a value  $S_k = 1$ . Conversely, if  $I_{P_k} < \alpha J_L L_P^2$ ,  $S_k = 0$ . We choose  $\alpha$  to be unity.

The total number of patches of size  $L_P$  in the ON-state is thus  $N_{\text{ON}}(L_P) = \sum_k S_k$ . If the entire LAFE glows and  $L_P$  is not too large, it is expected that  $N_{\text{ON}}(L_P) \sim L_P^{-2}$ . On the other hand, if the LAFE glows at the periphery, then  $N_{\text{ON}}(L_P) \sim L_P^{-1}$  provided  $L_P$  is small enough that bulk and surface effects can be distinguished.

Clearly, if  $L_P$  is too small, statistical errors are likely to be large, especially in the low field regime where a patch with only a few emitters may struggle to be in the ON state. On the other hand, if  $L_P$  is comparable to the size of the LAFE, saturation effects can set in. Thus, if a scaling exists, it must be in the intermediate region of patch size  $L_P$ . For convenience and comparison, the patch size  $L_P$  will be considered as integer multiples of

the mean separation  $c$  i.e.  $L_P = cN_C$ . Since the mean separation is  $c$ , the number of emitters in the patch of size  $L_P$  is the area of the patch  $L_P^2$  divided by the average area occupied by a single emitter,  $c^2$ . Thus the number of emitters in a patch of size  $L_P$  is  $L_P^2/c^2 = N_C^2$ .

## III. SCALING RESULTS

A typical random LAFE simulation starts with a random generation of  $N$  pin locations  $\{(x_i, y_i)\}$  distributed on a given shape having area  $Nc^2$ , using a uniform random number generator. This is followed by evaluation of  $\{\alpha_{S_i}\}$  and  $\{\gamma_i\}$  using Eq. (4). Once the individual enhancement factors are evaluated, the current from each pin can be determined and used to compute the total current, the average current density the current from a given ( $k^{\text{th}}$ ) patch of size  $L_P$  and the corresponding state  $S_k$ .

In the following, we shall consider LAFEs with hemi-ellipsoidal emitter pins of height  $h = 1500\mu\text{m}$  and base radius of curvature  $b = 12.5\mu\text{m}$ . This implies an apex radius of curvature  $R_a = b^2/h \approx 104.17\text{nm}^{38-40}$ . The number of emitters in the LAFE is typically  $3.6 \times 10^5$  and the mean separation  $c$  varies from  $1000\mu\text{m}$  to  $2500\mu\text{m}$ . Since the number of pins is held fixed, the LAFE area  $\mathcal{A}$  increases with  $c$ . Note that the dimensions considered here are not necessarily the typical ones involved in field emission but serve to illustrate the essential ideas of scaling.

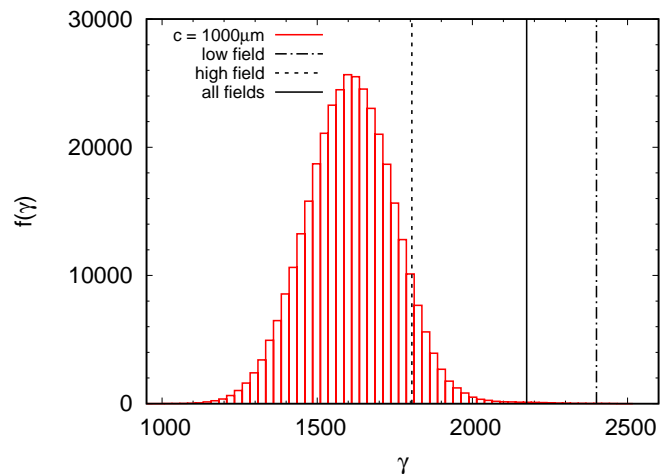


FIG. 1. The distribution of enhancement factors  $f(\gamma)$  at  $c = 1000\mu\text{m}$ ,  $h = 1500\mu\text{m}$  along with the characteristic values of  $\gamma$  extracted from an FN plot.

A typical frequency distribution of enhancement factors for  $c = 1000\mu\text{m}$  and  $h = 1500\mu\text{m}$  is shown in Fig. 1. The frequency distribution is obtained from the  $\{\gamma_i\}$  evaluated using Eq. (4) which is based on the line charge model. The vertical lines mark the extracted values of the characteristic enhancement factor from the FN plot ( $\ln(I/E_0^2)$  vs  $1/E_0$ ), assuming that  $B_L = B_{\text{FN}} \phi^{3/2} / \gamma_c$

where  $\gamma_c$  is the characteristic enhancement factor in the range of applied fields considered for the fit. The full range of applied field is  $E_0 \in [0.5, 3] \text{ V}/\mu\text{m}$ . Clearly, the low field and high field values of  $\gamma_c$  differ considerably and the FN-plot is nonlinear.

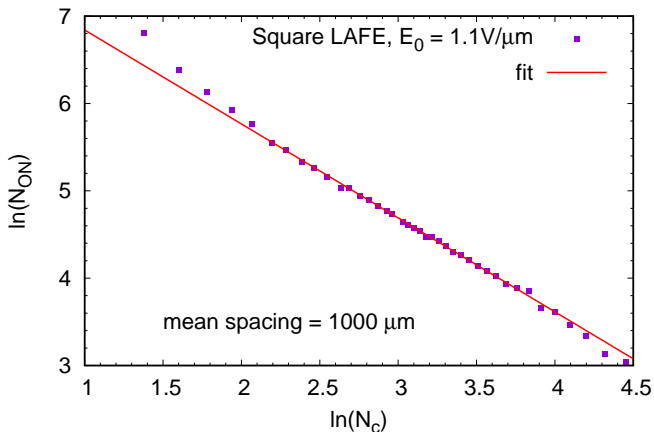


FIG. 2. Scaling behavior for a square LAFE with mean spacing  $c = 1000 \mu\text{m}$ . The number,  $N_{ON}$ , of patches in ON state scales as a power law with the patch length  $L_P = cN_C$ , as shown by the straight line fit.

The wide distribution of enhancement factors can lead to interesting local emission properties. Fig. 2 shows a typical  $\ln(N_{ON})$  vs  $\ln(N_C)$  plot for average inter-pin separation  $1000 \mu\text{m}$  at an applied field  $E_0 = 1.1 \times 10^{-3} \text{ V}/\text{nm}$  for a square LAFE. For intermediate patch size, the fit to a straight line is very good clearly indicating a power law scaling  $N_{ON} \sim L_P^{-D_e}$  where  $D_e$  is the slope of the fitted straight line. In this instance,  $D_e \approx 1.07$ , which is much smaller than 2. We shall hereafter refer to the scaling exponent  $D_e$  as the Emission-Dimension.

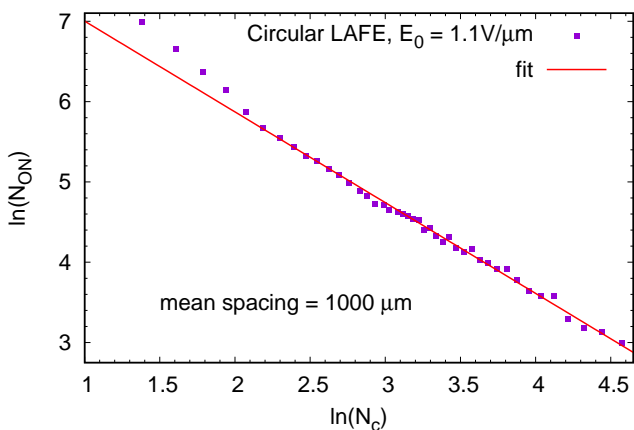


FIG. 3. Scaling behavior for a circular LAFE with mean spacing  $c = 1000 \mu\text{m}$ . The slope of the straight line is approximately -1.12.

A similar behavior is observed for a Circular LAFE. The number of patches in the ON state again scales as a

power law for  $E_0 = 1.1 \times 10^{-3} \text{ V}/\text{nm}$  and  $c = 1000 \mu\text{m}$ . In this case,  $D_e \approx 1.12$ . Since the number of emitters in the square and circle LAFE are the same, their net area is identical for a fixed  $c$ . Thus, if the area is  $L^2$ , the ratio of perimeter to area is  $4/L$  for a square LAFE. For a circle having area  $L^2$ , its radius is  $L/\sqrt{\pi}$  and the ratio of its circumference and area is  $(2\pi L/\sqrt{\pi})/L^2 = 2\sqrt{\pi}/L < 4/L$ . Thus, the square LAFE is more likely to have a peripheral glow pattern and hence the emission dimension is likely to be smaller. Note that for both the square and circular LAFE at  $E_0 = 1.1 \text{ V}/\mu\text{m}$ , the fit is in the range  $N_C \in [8, 90]$  corresponding to  $\ln(N_C) \in [2, 4.5]$ .

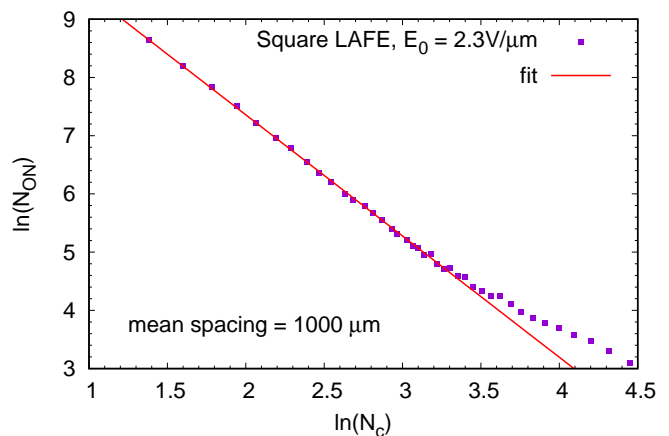


FIG. 4. Scaling behavior for a square LAFE at a higher applied field ( $E_0 = 2.3 \text{ V}/\mu\text{m}$ ).

The Emission-Dimension,  $D_e$ , should depend on the applied field  $E_0$  as well as the mean separation  $c$  between the emitters. Note that with an increase in applied field  $E_0$ , the small patch-size contributes in a manner similar to the intermediate patch size as seen in Fig. 4 where the straight line fit extends over  $N_C \in [4, 36]$  corresponding to  $\ln(N_C) \in [1.38, 3.6]$ . For purposes of determining the variation of  $D_e$  with  $E_0$ , we consider as a thumb rule a uniform intermediate range starting from  $\ln(N_C) \approx 2.2$  to  $\ln(N_C) \approx 3.6$  corresponding to  $N_C \in [9, 36]$ .

Fig. 5 shows the variation of the emission dimension  $D_e$  with the applied field  $E_0$  for three different LAFEs, having mean separation  $c$  equal to  $1000 \mu\text{m}$ ,  $1250 \mu\text{m}$ , and  $1500 \mu\text{m}$  respectively. Clearly,  $D_e \rightarrow 2$  for large  $E_0$  in all cases since the interior of the LAFE starts contributing substantially to the net emission current. A similar trend can be observed as the mean separation increases. For instance at  $E_0 = 1 \text{ V}/\mu\text{m}$ ,  $D_e$  increases from about 1 to 1.8 as the mean separation  $c$  increases from  $1000 \mu\text{m}$  to  $1250 \mu\text{m}$ . For  $c = 1500 \mu\text{m}$ ,  $D_e \approx 2.0$ . The rapid change is due to the sharp rise in the field enhancement factor with  $c$  and the change in  $f(\gamma)$  from being right-skewed to an almost symmetric distribution at  $c = 1500 \mu\text{m}$  as seen in Fig. 6.

Note that the extracted values of  $\gamma_c$  at low fields, high fields and the full range of applied field, are now more representative of the distribution. Moreover, the relative

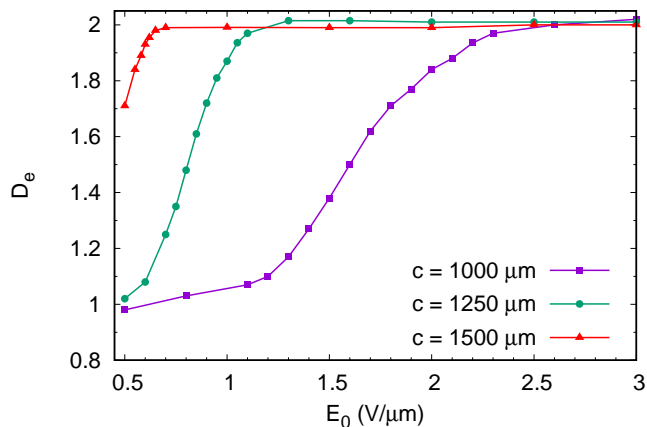


FIG. 5. Variation of the emission dimension  $D_e$  with applied electric field  $E_0$  for three separate mean separation ( $c$ ) of emitters.

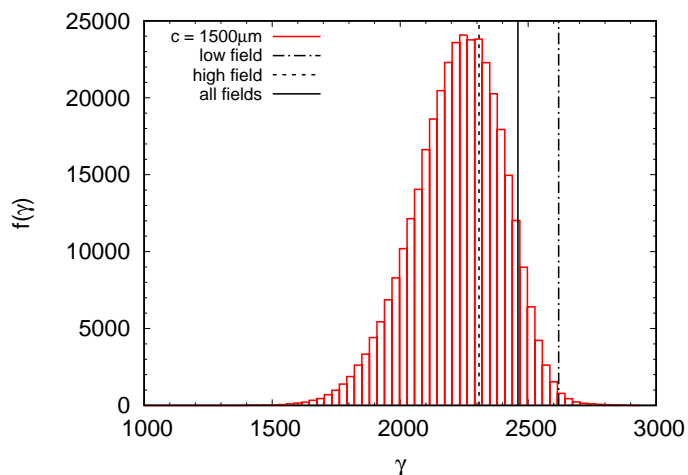


FIG. 6. The distribution of enhancement factors  $f(\gamma)$  at  $c = 1500\mu\text{m}$ ,  $h = 1500\mu\text{m}$  along with the characteristic values of  $\gamma$  extracted from an FN plot.

gap between the low and high field values is now smaller and as  $c$  increases further, the three values come closer and stand near the peak (mode). This also results in a linear FN-plot for the same range of applied fields and coincides with the emission dimension being  $D_e = 2$ .

#### IV. DISCUSSION AND SUMMARY

The study presented in this paper clearly establishes scaling properties of a large area field emitter and the existence of an emission dimension  $D_e$  that depends on the applied field. It is an especially useful characterization when emitters are tightly packed such that the mean spacing is smaller than the height of the emitter. This results in a large range of variation in  $D_e$  with the applied electric field.

While the theoretical study presented here was based

on vertically-standing emitters of identical height, the idea of scaling may be more generally applicable in large area field emitters and can be investigated both theoretically and (largely) experimentally.

The need to understand and characterize LAFEs beyond the conventional I-V analysis was motivated in part by recent experimental progress in studying local properties of a LAFE<sup>19,20,41,42</sup>. We believe, an equivalent experimental study of scaling in a large area field emitters is possible and will present us with a greater understanding of their emission properties and serve as a guide in designing practical devices.

*Acknowledgements:* The scaling study was taken up following a remark by Prof. G. Ravikumar on the emission properties of LAFE. The authors also acknowledge fruitful discussions with Dr. Raghendra Kumar.

*Data Availability:* The data that supports the findings of this study are available within the article.

#### V. REFERENCE

- <sup>1</sup>C. A. Spindt, J. Appl. Phys. 39, 3504 (1968).
- <sup>2</sup>C. A. Spindt, I. Brodie, L. Humphrey, and E. R. Westerberg, J. Appl. Phys. 47, 5248 (1976).
- <sup>3</sup>K. B. K. Teo, E. Minoux, L. Hudanski, F. Peauger, J. P. Schnell, L. Gangloff, P. Legagneux, D. Dieumegard, G. A. J. Amarantunga and W. I. Milne, Nature 437, 968 (2005).
- <sup>4</sup>F. Dams, A. Navitski, C. Prommesberger, P. Serbun, C. Langer, G. Muller, and R. Schreiner, IEEE Trans. Electron Devices 59, 2832 (2012).
- <sup>5</sup>R. J. Parmee, C. M. Collins, W. I. Milne, and M. T. Cole, Nano Convergence 2, 1 (2015).
- <sup>6</sup>A. Basu, M. E. Swanwick, A. A. Fomani, and L. F. Vela'squez-Garcia, J. Phys. D: Appl. Phys. 48, 225501 (2015).
- <sup>7</sup>D. R. Whaley, C. Armstrong, C. E. Holland, C. A. Spindt, and P. R. Schwoebel, in 31st International Vacuum Nanoelectronics Conference (IVNC) (IEEE, New York, 2018), p. 1.
- <sup>8</sup>J. R. Harris, K. L. Jensen, D. A. Shiffler, AIP Adv. 5 (2015) 087182.
- <sup>9</sup>J. R. Harris, K. L. Jensen, W. Tang, D. A. Shiffler, J. Vac. Sci. Technol. B 34 (2016) 041215.
- <sup>10</sup>D. Biswas, Phys. Plasmas 25, 043113 (2018).
- <sup>11</sup>D. Biswas and R. Rudra, Physics of Plasmas 25, 083105 (2018).
- <sup>12</sup>D. Biswas, Physics of Plasmas, 26, 073106 (2019).
- <sup>13</sup>R. Rudra and D. Biswas, AIP Advances, 9, 125207 (2019).
- <sup>14</sup>D. Biswas and R. Rudra, J. Vac. Sci. Technol. B, 38, 023207 (2020).
- <sup>15</sup>D. Biswas, J. Vac. Sci. Technol. B38, 063201 (2020).
- <sup>16</sup>T. A. de Assis, F. F. Dall'Agnol, and M. Cahay, Applied Physics Letters 116, 203103 (2020).
- <sup>17</sup>A. A. Al-Tabbakh, Ultramicroscopy, 218, 113087 (2020).
- <sup>18</sup>E. O. Popov, A. G. Kolosko, S. V. Filippov, T. A. de Assis, Vacuum, 173, 109159 (2020).
- <sup>19</sup>F. H. Read and N. J. Bowring, Nucl. Instrum. Methods Phys. Res. A 519, 305 (2004).
- <sup>20</sup>S. V. Filippov, A. G. Kolosko, R. M. Ryazanov, E. P. Kitsyuk, E. O. Popov, IOP Conference Series: Materials Science and Engineering 525, 012051 (2019).

- <sup>21</sup>R. G. Forbes, Appl. Phys. Lett. 92, 193105 (2008).
- <sup>22</sup>R. H. Fowler and L. Nordheim, Proc. R. Soc. A 119, 173 (1928).
- <sup>23</sup>L. Nordheim, Proc. R. Soc. A 121, 626 (1928).
- <sup>24</sup>R. E. Burgess, H. Kroemer, J. M. Houston, Phys. Rev. 90, 515 (1953).
- <sup>25</sup>E. L. Murphy and R. H. Good, Phys. Rev. 102, 1464 (1956).
- <sup>26</sup>K. L. Jensen, J. Vac. Sci. Technol. B 21, 1528 (2003).
- <sup>27</sup>R. G. Forbes, App. Phys. Lett. 89, 113122 (2006).
- <sup>28</sup>R. G. Forbes and J. H. B. Deane, Proc. R. Soc. A 463, 2907 (2007).
- <sup>29</sup>J. H. B. Deane and R. G. Forbes, J. Phys. A: Math. Theor. 41, 395301 (2008).
- <sup>30</sup>K. L. Jensen, *Introduction to the physics of electron emission*, Chichester, U.K., Wiley, 2018.
- <sup>31</sup>D. Biswas, G. Singh, S. G. Sarkar and R. Kumar, Ultramicroscopy 185, 1 (2018).
- <sup>32</sup>D. Biswas, G. Singh and R. Ramachandran, Physica E 109, 179 (2019).
- <sup>33</sup>D. Biswas, Physics of Plasmas 25, 043105 (2018).
- <sup>34</sup>R. G. Forbes, J. Vac. Sci. Technol. B 27, 1200 (2009).
- <sup>35</sup>C. J. Edgcombe, and U. Valdrè, Philosophical Magazine B 82, 987 (2002).
- <sup>36</sup>R. G. Forbes, C. J. Edgcombe, and U. Valdrè, Ultramicroscopy 95, 57 (2003).
- <sup>37</sup>D. Biswas, G. Singh and R. Kumar, J. Appl. Phys. 120, 124307 (2016).
- <sup>38</sup>For  $R_a < 100\text{nm}$ , curvature effects in the field emission current density become prominent and a different treatment is required. See [39 and 40].
- <sup>39</sup>D. Biswas and R. Ramachandran, J. Vac. Sci. Technol. B 37, 021801 (2019).
- <sup>40</sup>D. Biswas and R. Ramachandran, J. Appl. Phys. 129, 194303 (2021).
- <sup>41</sup>E. O. Popov, A. G. Kolosko, S. V. Filippov, and E. I. Terukov, J. Vac. Sci. Technol. B 36, 02C106 (2018).
- <sup>42</sup>E. O. Popov, A. G. Kolosko, S. V. Filippov, E. I. Terukov, R. M. Ryazanov, and E. P. Kitsyuk, J. Vac. Sci. Technol., B 38, 043203 (2020).